Proc. Natl. Acad. Sci. USA
Vol. 86, pp. 6148–6152, August 1989
Biophysics

High-order fluorescence fluctuation analysis of model protein clusters

(aggregation/autocorrelation/diffusion/fluorescence microscopy/receptor clustering)

ARTHUR G. PALMER III AND NANCY L. THOMPSON

Department of Chemistry, University of North Carolina, Chapel Hill, NC 27599-3290

Communicated by Robert G. Parr, May 25, 1989 (received for review April 12, 1989)

ABSTRACT **The technique of high-order fluorescence fluctuation autocorrelation for detecting and characterizing protein oligomers was applied to solutions containing two fluorescent proteins in which the more fluorescent proteins were analogues for clusters of the less fluorescent ones. The results show that the model protein clusters can be detected for average numbers of observed subunits (free monomers plus monomers in oligomers) equal to 10–100 and for relative fluorescent yields that correspond to oligomers as small as trimers. High-order fluorescent fluctuation analysis may therefore be applicable to cell surface receptor clusters in natural or model membranes.**

The formation of submicroscopic clusters of cell surface receptors has been implicated or confirmed as a key factor in intercellular communication for a variety of ligands and cell types (1–7). Information about protein–protein interactions in or on natural or model membranes has been obtained by measurements of intermolecular fluorescent energy transfer (8), protein translational (9) and rotational (10) mobility, electron microscopy (4), and gel electrophoresis (6). However, these techniques either rely on assumptions about the relationship of spectroscopic or hydrodynamic properties to molecular size or are not readily applicable to dynamic processes. New methods that monitor receptor clusters on the membranes of viable cells are needed to clarify the roles of clusters in membrane functions.

Digital video microscopy can characterize receptor clustering on viable cells if individual clusters are intensely fluorescent and sufficiently sparse to be optically resolved (11). If the clusters are less fluorescent or more densely distributed, the related technique of fluorescent correlation spectroscopy (12) can be employed. In this technique, movement of fluorescently labeled molecules through a small illuminated region generates temporal fluctuations in the fluorescence emitted from the region. The magnitude of the fluorescence fluctuation autocorrelation function is sensitive to the number densities and fluorescence yields of different fluorescent species. Recent experimental studies have demonstrated that fluorescence fluctuation analysis can detect protein aggregates in natural and model membranes, including virus glycoproteins on infected fibroblasts (13), acetylcholine receptors on developing muscle cells (14), and the membrane protein porin (15).

Only one parameter that directly depends on chemical composition (the magnitude of the fluorescence fluctuation autocorrelation function) is measured in conventional fluorescence correlation spectroscopy. High-order autocorrelation, which has recently attracted interest in a variety of theoretical and experimental contexts (16–19), is one method of obtaining additional independent information about oligomerization from the distribution of fluorescence fluctuations. Previous work has demonstrated that high-order fluorescence fluctuation autocorrelation functions can be measured for solutions of fluorescent lipid aggregates and that subsequent analysis yields reasonable values for the abundance and fluorescence yields of the aggregates (20). In the work described herein, the accuracy with which high-order fluorescence fluctuation autocorrelation can detect and quantify protein oligomerization has been rigorously evaluated using solutions containing two fluorescent proteins.

THEORETICAL BACKGROUND

Monomers and oligomers are simulated by two different fluorescent proteins of concentrations C_m and C_o, respectively. The fluorescence yield of the model oligomers relative to the model monomers, denoted by $\alpha > 1$, is assumed to equal the oligomeric stoichiometry. The total concentration of monomeric protein subunits (C_t) and the fraction of the protein monomers that are present in oligomeric form (f) are given by

$$C_t = C_m + \alpha C_o, \quad [1]$$

$$f = \alpha C_o / C_t. \quad [2]$$

High-order fluorescence fluctuation autocorrelation functions are defined as (20)

$$G_{i,j}(\tau) = \frac{\langle \delta F^i(t+\tau)\delta F^j(t)\rangle - \langle \delta F^i(t)\rangle\langle \delta F^j(t)\rangle}{\langle F(t)\rangle^{i+j}}, \quad [3]$$

where $\delta F(t) = F(t) - \langle F\rangle$ is the fluctuation of the fluorescence at time t from its average value, i and j are integers, and $\langle\ \rangle$ denotes a thermodynamic ensemble average. For samples in equilibrium, $G_{i,j}(\tau) = G_{j,i}(\tau)$. $G_{1,1}(\tau)$ is the conventional autocorrelation function.

For samples containing two fluorescent components, the magnitudes of the lowest-order autocorrelation functions are (20)

$$G_{1,1}(0) = \gamma_2\beta_2$$

$$G_{1,2}(0) = \gamma_3\beta_3$$

$$G_{2,2}(0) = \gamma_4\beta_4 + 2\gamma_2^2\beta_2^2$$

$$G_{1,3}(0) = \gamma_4\beta_4 + 3\gamma_2^2\beta_2^2, \quad [4]$$

The publication costs of this article were defrayed in part by page charge payment. This article must therefore be hereby marked "*advertisement*" in accordance with 18 U.S.C. §1734 solely to indicate this fact.

Abbreviations: BPE, B-phycoerythrin; R-IgG, IgG labeled with tetramethylrhodamine isothiocyanate; B-IgG, IgG labeled with fluorescein–rhodamine bifluorophore FR-1.

Table 1. Mixture compositions

Sample	C_m	C_o	C_t	f
Mixture A (C_m = [R-IgG], C_o = [BPE], α = 28.3)				
1	25.7	0.241	32.5	0.210
2	25.7	0.361	35.9	0.285
3	15.4	0.361	25.6	0.399
4	7.72	0.241	14.5	0.470
5	7.72	0.361	17.9	0.571
6	7.72	0.602	24.8	0.687
7	2.57	0.361	12.8	0.798
Mixture B (C_m = [B-IgG], C_o = [BPE], α = 20.5)				
1	74.4	0.241	79.3	0.062
2	37.2	0.241	42.1	0.117
3	37.2	0.361	44.6	0.166
4	22.3	0.361	29.7	0.249
5	11.1	0.241	16.0	0.309
6	11.1	0.361	18.5	0.400
7	11.1	0.602	23.4	0.527
Mixture C (C_m = [R-IgG], C_o = [B-IgG], α = 3.46)				
1	11.2	0.742	13.8	0.186
2	5.58	0.445	7.12	0.216
3	11.2	1.11	15.0	0.256
4	5.58	0.742	8.15	0.315

Shown are the solution compositions that mimic mixtures of monomeric and oligomeric proteins. The values of C_t and f were calculated (Eqs. 1 and 2) from the known values of C_m, C_o, and α (see *Materials and Methods*). Concentrations are in molecules per μm^3; relative uncertainties in concentrations and α are ≈10%.

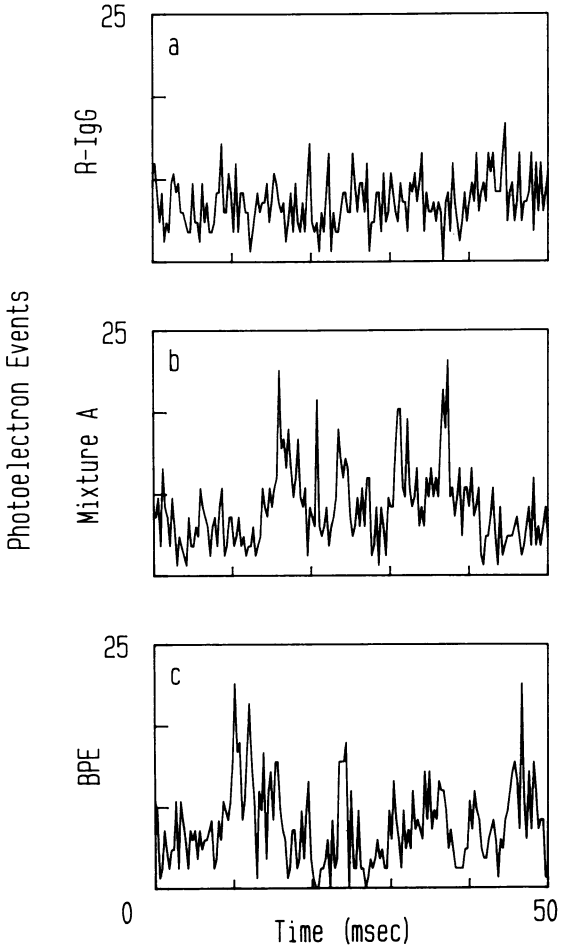

FIG. 1. Photoelectron fluctuations. Shown are short segments of the experimentally measured photoelectron counts for R-IgG at 18 molecules per μm^3 (*a*), a mixture of R-IgG at 7.8 molecules per μm^3 and BPE at 0.36 molecule per μm^3 (*b*), and BPE at 0.60 molecule per μm^3 (*c*).

where

$$\beta_n = \frac{C_m + \alpha^n C_o}{C_t^n} = \frac{1 - f + \alpha^{n-1} f}{C_t^{n-1}}, \quad [5]$$

$$\gamma_n = \left[\int_{\Omega_o} W^n(\mathbf{r})\, d^3r\right] \Big/ \left[\int_{\Omega_o} W(\mathbf{r})\, d^3r\right]^n, \quad [6]$$

the function $W(\mathbf{r})$ is the product of the spatial intensity profile of the excitation light and the spatial detection efficiency, and Ω_o is the sample extent. Experimentally, the values of β_n are obtained from the measured values of γ_n and $G_{i,j}(0)$ for $i + j \leq n$ and provide information about the degree and stoichiometry of oligomerization.

Sample heterogeneity can be *detected* by calculating the quantities

$$r_n = \beta_n^{1/(n-1)}/\beta_2 \qquad (n \geq 3), \quad [7]$$

which are greater than unity only if more than one fluorescent species is present, regardless of the number of components, the distribution of oligomer sizes, the degree of fluorescence yield changes in clusters, or the total concentration of mo-

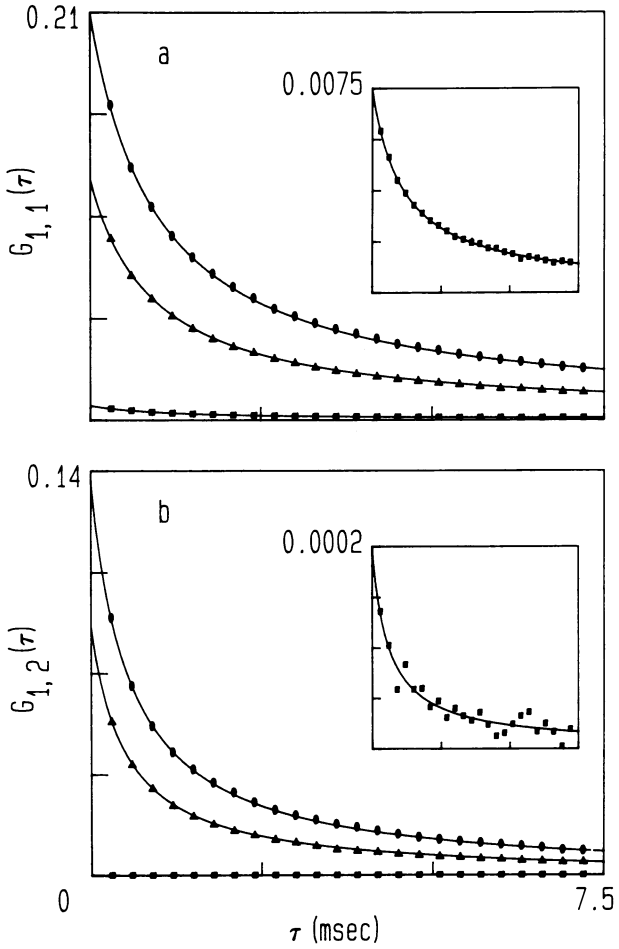

FIG. 2. High-order fluorescence fluctuation autocorrelation functions. Shown are the values of $G_{1,1}(\tau)$ and $G_{1,2}(\tau)$ (*a* and *b*, respectively) for R-IgG at 18 molecules per μm^3 (■), a mixture of R-IgG at 7.8 molecules per μm^3 and BPE at 0.36 molecule per μm^3 (▲), and BPE at 0.60 molecule per μm^3 (●) obtained by correcting the experimentally obtained photoelectron fluctuation autocorrelation functions for stochastic photon collection and detection and for background intensity. (*Insets*) Functions for R-IgG at 18 molecules per μm^3 expanded to full scale. Solid lines are the best fits to Lorentzians in $\tau^{1/2}$.

nomeric molecules (23). Sample heterogeneity can be *quantified* by analyzing the values of the measured β_n, which are different functions of C_m, C_o, and α and therefore contain independent information about the extent of oligomerization. Eq. 5 contains three unknown, independent parameters (e.g., f, α, and C_t, or C_m, C_o, and α). Therefore, measured values of β_2, β_3, and one additional parameter, or measured values of β_2, β_3, and β_4, should yield values for the other variables.

MATERIALS AND METHODS

Solutions contained one or two of the following proteins in phosphate-buffered saline (0.05 M sodium phosphate/0.14 M NaCl/0.01% NaN_3, pH 7.4): B-phycoerythrin (BPE, Molecular Probes), IgG (sheep, Sigma) labeled with tetramethylrhodamine isothiocyanate (Molecular Probes) (R-IgG), and IgG labeled with fluorescein–rhodamine bifluorophore FR-1 (Molecular Probes) (B-IgG). The solutions also contained 1 μM unlabeled IgG to reduce adsorption to glass surfaces. Three mixtures were examined: mixture A, BPE and R-IgG; mixture B, BPE and B-IgG; mixture C, R-IgG and B-IgG.

Solutions of fluorescent proteins were mounted on a fluorescence microscope constructed from an optical microscope (Zeiss IM-25), an argon ion laser (Coherent Innova 90-3), and a single-photon counting photomultiplier (RCA 31034A) as described (20–22). The sample volume was defined by the laser beam as focused through a spatial filter and a ×60, 1.4 n.a. microscope objective and by a 50-μm-radius pinhole in an image plane between the sample and detector. Laser conditions were as follows: mixture A, 514.5 nm, 5 μW; mixture B, 488.0 nm, 10 μW; mixture C, 488.0 nm, 50 μW. The radius of the laser beam was 0.44 ± 0.06 μm (514.5 nm) or 0.48 ± 0.07 μm (488.0 nm) and the sample volume was ≈1.2 μm^3 (514.5 nm) or ≈1.6 μm^3 (488.0 nm) (21).

Photoelectron fluctuations were recorded as the number of events per 10^6 consecutive sample times of 0.3-ms duration. High-order photoelectron fluctuation autocorrelation functions were calculated from the digital records of photoelectron counts per sample interval and were fit with theoretical functions for a system characterized by a single diffusion time (20, 22). Values of $G_{i,j}(0)$ were determined by correcting the extrapolated time-zero values of the photoelectron fluctuation autocorrelation functions for stochastic photon collection and detection and for background intensity as described (22).

BPE concentrations were determined spectrophotometrically and monodisperse BPE solutions were then used to measure the constants γ_2, γ_3, and γ_4, which depend only on

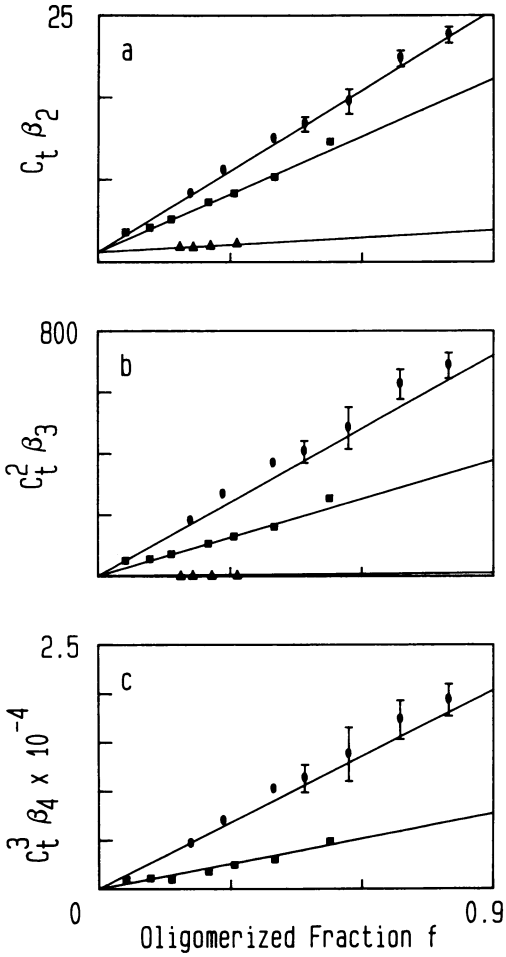

FIG. 3. Constants β_n for monodisperse and polydisperse solutions. Shown are $C_t\beta_2$ (*a*), $C_t^2\beta_3$ (*b*), and $C_t^3\beta_4$ (*c*) for mixtures A (●), B (■), and C (▲) as functions of the "oligomerized" fraction f. The values of β_n were determined from high-order fluorescence fluctuation analyses, and C_t and f values are from Table 1. Solid lines give the values of the parameters expected for the known concentrations and fluorescence yields of the two species. Error bars give the standard errors in the means of three independent measurements; error bars that are smaller than the symbol are not shown.

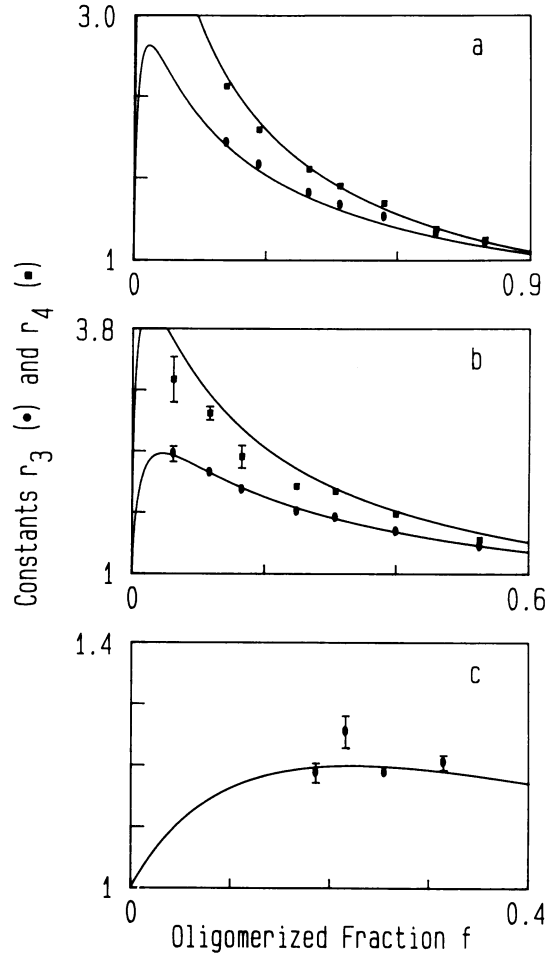

FIG. 4. Constants r_n for monodisperse and polydisperse solutions. Shown are the experimentally determined values of the constants r_3 (●) and r_4 (■) for mixtures A (*a*), B (*b*), and C (*c*) as functions of the "oligomerized" fraction f as shown in Table 1. Solid lines give the values of the parameters expected for the independently measured concentrations and fluorescence yields of the two species. Error bars give the standard errors in the means of three independent measurements; error bars that are smaller than the symbol are not shown.

the wavelength of the excitation light and the geometry of the optical apparatus (21). Concentrations of fluorescently labeled IgG were determined from the known values of γ_2 and the measured values of $G_{1,1}(0)$ for monodisperse IgG solutions (Eqs. 4 and 5). The relative fluorescence yields (α) of the model oligomers were determined from the concentration dependence of the fluorescence intensities of monodisperse solutions.

RESULTS AND DISCUSSION

As shown in Table 1, the sample compositions simulated a variety of total monomer concentrations and degrees and stoichiometries of oligomerization. The more fluorescent proteins modeled oligomers of 28 (mixture A), 20 (mixture B), or 3 (mixture C) subunits of the less fluorescent proteins. The values of f corresponded to the full range of fractional oligomerization and the values of C_t corresponded to 10–100 molecules in sample volumes of $\approx 1\ \mu m^3$. Assuming a typical sample area for cell membranes of $\approx 0.25\ \mu m^2$ for illumination with an ≈ 0.4-μm-radius laser beam, the receptor densities modeled are therefore 40–400 molecules per μm^2, which are typical concentrations for cell surface receptors.

Fig. 1 shows representative segments of the photoelectron events recorded for three different samples of mixture A. Solution compositions were chosen so that [R-IgG] + α[BPE] was approximately constant and the set modeled solutions containing equal total protein concentrations in monomeric (Fig. 1*a*), partially oligomeric (Fig. 1*b*), or completely oligomeric (Fig. 1*c*) states. As shown, the photoelectron fluctuations have similar temporal characteristics but the relative magnitudes of the fluctuations are larger for the samples that contain model oligomers. Photoelectron fluctuations for B-IgG and for mixtures B and C appeared similar.

Fig. 2 shows typical high-order fluorescence fluctuation autocorrelation functions calculated from the photoelectron records of the samples shown in Fig. 1. The presence of the model oligomers dramatically increases the magnitude of these functions compared to the magnitudes for monomer solutions. Blank solutions of unlabeled IgG in phosphate-buffered saline showed no correlations on the time scale of interest.

The constants γ_n were determined from the dependence of the magnitudes of $G_{i,j}(0)$ on the spectrophotometrically calibrated concentration of monodisperse BPE solutions as described (21). The measured values of γ_n agreed with theoretical predictions (21) and were as follows: 514.5 nm, $\gamma_2 = 0.144 \pm 0.010\ \mu m^{-3}$, $\gamma_3 = 0.062 \pm 0.005\ \mu m^{-6}$, $\gamma_4 = 0.034 \pm 0.003\ \mu m^{-9}$; 488.0 nm, $\gamma_2 = 0.111 \pm 0.006\ \mu m^{-3}$, $\gamma_3 = 0.039 \pm 0.003\ \mu m^{-6}$, $\gamma_4 = 0.017 \pm 0.001\ \mu m^{-9}$.

The measured values of γ_n were used to determine the β_n from the $G_{i,j}(0)$ according to Eq. 4. As shown in Fig. 3, the quantities $C_t^{n-1}\beta_n$ were linearly dependent on the fractional oligomerization f as predicted by Eq. 5, and the experimental values of β_n agreed with values calculated from the known solution compositions given in Table 1. The values of β_4 for mixture C could not be reproducibly measured because of the low absolute fluorescence intensity for these samples (at 50 μW and 488.0 nm) and are therefore not reported.

The β_n were then used to calculate the r_n according to Eq. 7. As shown in Fig. 4, all mixture samples had $r_3 > 1$ within statistical accuracy and the measured values of r_3 compared well with the values predicted by Eqs. 5 and 7 for the known values of α, C_m, and C_o. In addition, all single-component, monodisperse samples had $r_3 = 1$ within statistical accuracy; the measured values were 1.014 ± 0.003, 1.02 ± 0.01, and 1.00 ± 0.03 for BPE, B-IgG, and R-IgG, respectively. In addition, mixtures A and B had $r_4 > 1$ and solutions of BPE and B-IgG had r_4 values of 1.008 ± 0.005 and 1.03 ± 0.06, respectively. The values of r_4 for monodisperse R-IgG and for mixture C could not be reproducibly measured and are not reported. Thus, the parameter r_3 is a simple test for the presence of polydispersity or oligomerization that will be accurate for values of $3 \leq \alpha \leq 30$, and possibly for other oligomerization stoichiometries, and r_4 will yield confirming evidence for values of $\alpha \approx 20$.

In many systems, the total concentration of receptor subunits C_t can be determined with fair accuracy and then used with the measured values of β_2 and β_3 to calculate C_m, C_o, and α by using Eq. 5. As an example, the effective value

Table 2. Model protein oligomers detected by fluorescence fluctuation analysis

Sample	C_m	C_o	α	C_t	f
		Mixture A (C_m = [R-IgG], C_o = [BPE])			
1	23.5 ± 0.2	0.22 ± 0.01	27.0 ± 0.9	29.4 ± 0.3	0.200 ± 0.002
2	24.2 ± 0.4	0.31 ± 0.01	29.0 ± 1.0	33.1 ± 0.9	0.267 ± 0.008
3	15.7 ± 0.6	0.31 ± 0.01	30.7 ± 0.8	25.3 ± 0.7	0.381 ± 0.008
4	8.3 ± 0.3	0.21 ± 0.01	30.8 ± 0.9	14.9 ± 0.3	0.444 ± 0.011
5	8.3 ± 0.2	0.31 ± 0.02	29.4 ± 2.6	17.3 ± 0.6	0.518 ± 0.017
6	8.3 ± 0.2	0.53 ± 0.02	30.0 ± 0.9	24.1 ± 0.8	0.656 ± 0.008
7	3.1 ± 0.1	0.32 ± 0.01	29.5 ± 1.1	12.5 ± 0.2	0.753 ± 0.010
		Mixture B (C_m = [B-IgG], C_o = [BPE])			
1	70.9 ± 1.0	0.30 ± 0.05	23.6 ± 1.6	77.7 ± 0.5	0.088 ± 0.010
2	37.9 ± 0.3	0.25 ± 0.02	21.5 ± 0.7	43.3 ± 0.4	0.125 ± 0.005
3	35.1 ± 1.2	0.37 ± 0.04	19.4 ± 1.3	42.2 ± 1.2	0.168 ± 0.006
4	21.6 ± 0.4	0.40 ± 0.02	19.7 ± 0.6	29.4 ± 0.3	0.266 ± 0.007
5	10.9 ± 0.2	0.24 ± 0.02	20.2 ± 0.3	15.7 ± 0.5	0.303 ± 0.013
6	11.7 ± 0.3	0.37 ± 0.01	21.2 ± 0.2	19.6 ± 0.2	0.402 ± 0.010
7	11.0 ± 0.1	0.59 ± 0.02	22.3 ± 0.4	24.2 ± 0.4	0.543 ± 0.010
		Mixture C (C_m = [R-IgG], C_o = [B-IgG])			
1	10.1 ± 0.4	0.70 ± 0.16	3.4 ± 0.2	12.5 ± 0.2	0.186 ± 0.030
2	5.5 ± 0.1	0.26 ± 0.05	4.1 ± 0.3	6.5 ± 0.1	0.159 ± 0.019
3	10.3 ± 0.3	1.00 ± 0.16	3.4 ± 0.1	13.6 ± 0.3	0.245 ± 0.033
4	5.1 ± 0.2	0.57 ± 0.06	3.6 ± 0.1	7.2 ± 0.1	0.285 ± 0.021

Shown are the values of C_o, C_m, α, and f determined from fluorescence fluctuation analysis, which are in good agreement with the known values shown in Table 1. C_t was measured by calibrating the mean fluorescence intensity; α and f were determined from C_t together with β_2 and β_3 from $G_{1,1}(0)$, $G_{1,2}(0)$, and $G_{2,1}(0)$; C_m and C_o were determined from C_t, α, and f according to Eqs. 1 and 2. Uncertainties shown are the standard errors in the means of three independent measurements.

of C_t for the model solutions was determined by comparing the fluorescence intensities of the mixture solutions with those of monomer protein solutions. As shown by comparing Tables 1 and 2, the concentrations and relative fluorescence yields obtained using experimentally determined values of β_2, β_3, and C_t were in surprisingly good agreement with the known values, given the visual similarity of the unprocessed photoelectron fluctuations (Fig. 1). In other experimental systems, different auxiliary information such as the relative fluorescence yield α may be available, which will enable two of the variables in Eq. 5 to be determined from β_2 and β_3. The parameter values (C_m, C_o, C_t, and f) determined by this alternative analysis were also in good agreement with the known values (23).

Theoretically, the measured values of β_2, β_3, and β_4 should allow determination of the three independent parameters in Eq. 5. However, in the present work, quantitative analyses that employed β_4 were not successful. This limitation appears to result from uncertainty in the measured value of γ_4 ($\approx$10%), which is propagated to the measured value of β_4. In two-dimensional samples, the value of $\gamma_4^{1/2}$ should be $\approx$4 μm^{-3} for excitation with a Gaussian-shaped laser beam of radius $\approx$0.4 μm (21) in contrast to the value of $\gamma_4^{1/3} \approx 0.3$ μm^{-3} for bulk samples. Thus, the fractional uncertainty in γ_4 may be lower for membranes, and analyses that employ β_4 in addition to β_2 and β_3 might be more accurate.

Elucidation of the mechanism and function of cell surface receptor clustering requires experimental techniques that are sensitive to the formation of molecular aggregates. The work described here demonstrates that high-order fluorescence fluctuation autocorrelation can provide accurate information on the concentrations of oligomers in the presence of monomers. The method does not require sample fixation or assumptions about the relationship of transport properties to molecular size and is accurate for chemical compositions appropriate to cell surface receptors. Applications to natural or model membranes should provide new and independent information about the roles of cell surface receptor clusters in the functions of biological membranes.

We thank Richard and Rosario Haugland (Molecular Probes) for generously providing fluorescein–rhodamine bifluorophore-labeled IgG. This work was supported by National Institutes of Health Grant GM37145, by National Science Foundation Presidential Young Investigator Award DCB-8552986, and by E. I. DuPont de Nemours.

1. Davies, D. R. & Metzger, H. (1983) *Annu. Rev. Immunol.* **1,** 87–117.
2. Young, J. D., Unkeless, J. C., Young, T. M., Mauro, A. & Cohn, Z. A. (1983) *Nature (London)* **306,** 186–189.
3. Axelrod, D., Ravdin, P., Koppel, D. E., Schlessinger, J., Webb, W. W., Elson, E. L. & Podleski, T. R. (1976) *Proc. Natl. Acad. Sci. USA* **73,** 4594–4598.
4. Abney, J. R., Braun, J. & Owicki, J. C. (1987) *Biophys. J.* **52,** 441–454.
5. Cuatrecasas, P. (1983) *Drug Intell. Clin. Pharmacol.* **17,** 357–366.
6. Yarden, Y. & Schlessinger, J. (1987) *Biochemistry* **26,** 1443–1451.
7. Williams, L. T. (1989) *Science* **243,** 1564–1570.
8. Watts, T. H., Gaub, H. E. & McConnell, H. M. (1986) *Nature (London)* **320,** 179–181.
9. Wright, L. L., Palmer, A. G. & Thompson, N. L. (1988) *Biophys. J.* **54,** 463–470.
10. Velez, M. & Axelrod, D. (1988) *Biophys. J.* **53,** 575–591.
11. Gross, D. & Webb, W. W. (1986) *Biophys. J.* **49,** 901–911.
12. Magde, D., Elson, E. L. & Webb, W. W. (1974) *Biopolymers* **13,** 29–61.
13. Petersen, N. O., Johnson, D. C. & Schlesinger, M. J. (1986) *Biophys. J.* **49,** 817–820.
14. Velez, M. & Axelrod, D. (1988) *Biophys. J.* **53,** 638 (abstr.).
15. Meyer, T. & Schindler, H. (1988) *Biophys. J.* **54,** 983–993.
16. Suck, J. B., Quitman, D. & Maier, B., eds. (1985) *J. Phys.* **46(C9).**
17. Lohman, A. W. & Wirnitzer, B. (1984) *Proc. IEEE* **72,** 889–901.
18. Leibovitch, L. S., Fischbarg, J. & Koniarek, J. P. (1985) *Math. Biosci.* **76,** 1–13.
19. Blumich, B. (1987) *Rev. Sci. Instrum.* **58,** 911–919.
20. Palmer, A. G. & Thompson, N. L. (1987) *Biophys. J.* **52,** 257–270.
21. Palmer, A. G. & Thompson, N. L. (1989) *Appl. Opt.* **28,** 1214–1220.
22. Palmer, A. G. & Thompson, N. L. (1989) *Rev. Sci. Instrum.* **60,** 624–633.
23. Palmer, A. G. (1989) Ph.D. Thesis (Univ. of North Carolina, Chapel Hill).